Astron. Astrophys. 338, L55–L58 (1998)

ASTRONOMY AND ASTROPHYSICS

LETTER

Letter to the Editor

Simulations of an alpha-effect due to magnetic buoyancy

Axel Brandenburg[1] **and Dieter Schmitt**[2]

[1] Department of Mathematics, University of Newcastle upon Tyne, NE1 7RU, UK
[2] Universitäts-Sternwarte Göttingen, Geismarlandstrasse 11, D-37083 Göttingen, Germany

Received 20 July 1998 / Accepted 20 August 1998

Abstract. Three-dimensional simulations of a thermally stably stratified gas with a localized layer of toroidal magnetic field are carried out. The magnetic field gives rise to a magnetic buoyancy instability. Due to the presence of rotation the resulting fluid motions are helical and lead to an α-effect, i.e. to a component of the electromotive force in the direction of the mean magnetic field. The value of α is estimated during the exponential growth phase of the instability. The mean vertical transport velocity of the magnetic field is also calculated. It is found that α varies with latitude and its value is positive in the northern hemisphere.

Key words: Sun: magnetic fields – magnetohydrodynamics – dynamo – instabilities

1. Introduction

The concept of an α-effect invoked to explain the origin of large scale magnetic fields in rotating astrophysical bodies has a long-standing history since the seminal papers by Parker (1955) and Steenbeck, Krause & Rädler (1966). The original idea was that cyclonic or helical background fluid motions $\boldsymbol{u}$ could distort the magnetic field $\boldsymbol{B}$ such that the resulting average electromotive force, $\langle \boldsymbol{u} \times \boldsymbol{B} \rangle$, has a component $\alpha \langle \boldsymbol{B} \rangle$ in the direction of the mean magnetic field, $\langle \boldsymbol{B} \rangle$. The coefficient α represents the α-effect (Moffatt 1978, Krause & Rädler 1980).

There is now increasing evidence that, once the field has reached appreciable strength, the relevant fluid motions may result from the magnetic field itself or, more specifically, from magnetic instabilities. Thus, the velocity field that provides the α-effect is directly dependent on the magnetic field. Of major interest recently has been the Balbus-Hawley (1991) instability, relevant to explain turbulence in accretion discs. The three-dimensional simulations of Brandenburg et al. (1995, hereafter referred to as BNST) have shown that large scale magnetic fields can be generated from the fluid motions associated with this instability.

In the context of the solar dynamo the dominant instability could be a magnetic buoyancy instability. This possibility was first proposed by Moffatt (1978) and explored in detail by Schmitt (1984, 1985). He considered, in the magnetohydrodynamically rapidly rotating limit, a localized magnetic layer with a toroidal field in the overshoot region at the base of the convection zone. The upper parts of the layer, where the magnetic field decreases rapidly enough with height, are unstable due to magnetic buoyancy. In this buoyancy instability potential energy of extra mass supported against gravity is released by downward transport of mass and upward transport of magnetic flux. Because of rotation the instability takes the form of magnetostrophic waves where the Coriolis force and the Lorentz force are in approximate balance with each other. These waves are helical; their growth in amplitude causes a phase shift between the magnetic field and velocity perturbations, which leads to a component of the electromotive force parallel or antiparallel to the background toroidal field. This dynamic α-effect operates in strong fields which resist distortion by convective flows. In Schmitt's linear asymptotic analysis there are always two magnetostrophic modes with the same growth rate but with a north- and a southward component of phase velocity, respectively. Superposition of the most unstable modes leads to a non-monotonic latitudinal dependence, with α negative near the equator and positive near the pole in the northern hemisphere. However, α remains always antisymmetric with respect to the equator.

Related investigations have recently been carried out by Thelen (1997). An α-effect has also been derived from an instability of thin magnetic flux tubes (Ferriz-Mas et al. 1994, see also Hanasz & Lesch 1997). An application to the solar dynamo can be found in Schmitt et al. (1996). Estimates for turbulent magnetic diffusion due to the Parker instability have been given by Hasler et al. (1995), who used two-dimensional simulations without rotation.

In this Letter we present some exploratory three-dimensional simulations of an α-effect due to magnetic buoyancy using the code and setup described in Brandenburg et al. (1996, hereafter referred to as BJNRST). The governing equations are the continuity equation, the momentum equation with vertical gravity, Coriolis, Lorentz and viscous forces, the energy equation and the induction equation. For the full set of equations and details of the model we refer to BJNRST. Unlike Schmitt's original work we do not adopt the anelastic approximation, nor do we neglect the inertia term in the momentum equation. However, it would be computationally expensive to approach the limiting magnetostrophic regime of Schmitt (1985), who considered the ordering

$$\tau_{\rm ac} \ll \tau_\Omega \ll \tau_{\rm A} \ll \tau_{\rm ms} \tag{1}$$

of acoustic, rotational, Alfvén and magnetostrophic time scales, respectively. The magnetostrophic time scale is given by $\tau_{\rm ms}=\tau_{\rm A}^2/\tau_\Omega$. In the present work we restrict ourselves to the ordering

$$\tau_{\rm ac} \sim \tau_\Omega < \tau_{\rm A} < \tau_{\rm ms}. \tag{2}$$

Our main objective is to establish the existence of an α-effect, as well as its sign and latitudinal dependence.

2. The model

2.1. Basic setup and parameters

We use the code of BJNRST in a rectangular domain $|x|<L_x/2$, $|y|<L_y/2$ and $|z|\le L_z/2$, where $\boldsymbol{x}$ points north, $\boldsymbol{y}$ east, and $\boldsymbol{z}$ increases downwards. The linear analysis by Schmitt (1985) suggests that the most rapidly growing eigenmode should be well accommodated if the box aspect ratios satisfy $L_x<L_z<L_y$. We thus take $L_x=0.5$, $L_y=5$, $L_z=1$ for all our models using $31\times31\times64$ meshpoints.

We use periodic boundary conditions in the x and y directions and stress-free boundary conditions in the z direction. The x and y components of the magnetic field are assumed to vanish at $z=\pm L_z/2$. At the top of the box ($z=-L_z/2$) the temperature is such that the local pressure scale height at the top, H_{p0}, is equal to the height of the box. At the bottom ($z=+L_z/2$) the temperature gradient (proportional to the radiative flux) is given.

We assume a perfect gas with the ratio of specific heats being 5/3. The basic state is a polytrope with polytropic index $m=3$, corresponding to stable stratification in the absence of a magnetic field. The initial temperature profile is linear, but the density profile is modified such that the initial state is in hydrostatic equilibrium. We use nondimensional variables such that $H_{p0}=g=\overline{\rho}=\mu_0=c_p=1$, where $\overline{\rho}$ is the average density of the gas in the box. (So time is measured in units of $(H_{p0}/g)^{1/2}$, length in units of H_{p0}, and the magnetic field in units of $(\mu_0\overline{\rho}H_{p0}g)^{1/2}$.) To characterize a particular simulation we use the nondimensional parameters of BJNRST. In practice we fix the value of the rotational time scale, $\tau_\Omega=(2\Omega)^{-1}$ in terms of the acoustic time scale, $\tau_{\rm ac}=H_{p0}/c_{\rm s0}=\sqrt{H_{p0}/g}$, where $c_{\rm s0}$ is the isothermal sound speed at the top of the box. The ratio $\tau_{\rm ac}/\tau_\Omega$ is related to Taylor, Rayleigh and Prandtl numbers, Ta, Ra and Pr, respectively, via

$$\left(\frac{\tau_{\rm ac}}{\tau_\Omega}\right)^2=\frac{(2\Omega)^2}{g/H_{p0}}=-\frac{2}{15}\,\frac{\rm Pr\,Ta}{\rm Ra}. \tag{3}$$

Unless stated otherwise, the nondimensional parameters of BJNRST are $\rm Ra=-10^6$, $\rm Ta=7.5\times10^6$, and $\rm Pr=Pr_{\it M}=1$.

The initial magnetic field is given by $\boldsymbol{B}=(0,B_y,0)$ with

$$B_y=v_{\rm A0}\,\exp[-(z/H_{\rm B})^2], \tag{4}$$

where $H_{\rm B}=0.3$ is the scale height of the magnetic field. For most of our runs we take $v_{\rm A0}/c_{\rm s0}=0.3$, so $\tau_{\rm A}/\tau_{\rm ac}=(v_{\rm A0}/c_{\rm s0})^{-1}\sim3$. This corresponds to a Lundquist number, $v_{\rm A0}H_{p0}/\eta$, of 820.

2.2. Calculation of alpha

We restrict ourselves to estimating only those transport coefficients that involve the initial toroidal magnetic field, $\langle B_y\rangle$. We assume that we can represent the mean electromotive force, $\boldsymbol{\mathcal{E}}=\langle\boldsymbol{u}\times\boldsymbol{b}\rangle$, where $\boldsymbol{u}$ and $\boldsymbol{b}$ are fluctuations, in the form

$$\boldsymbol{\mathcal{E}}\approx\alpha\langle\boldsymbol{B}\rangle+\gamma\hat{\boldsymbol{z}}\times\langle\boldsymbol{B}\rangle-\eta_t\boldsymbol{\nabla}\times\langle\boldsymbol{B}\rangle, \tag{5}$$

where η_t is turbulent magnetic diffusion and γ measures the magnitude and direction of an average transport velocity of the mean magnetic field (sometimes called the γ-effect, see Krause & Rädler 1980). We take averages, $\langle...\rangle$, over the entire box. Since we use periodic and zero horizontal field boundary conditions in the horizontal and vertical directions, respectively, all derivatives of averages vanish. In particular we have $\boldsymbol{\nabla}\times\langle\boldsymbol{B}\rangle=0$. Therefore $\boldsymbol{\mathcal{E}}$ depends in our case only on α and γ. Since the main contribution to $\langle\boldsymbol{B}\rangle$ comes from the toroidal component of $\langle\boldsymbol{B}\rangle$, we have $\alpha\sim\mathcal{E}_y/\langle B_y\rangle$ and $\gamma\sim-\mathcal{E}_x/\langle B_y\rangle$.

We note that Hasler et al. (1995) used horizontal averages and found both γ and η_t from their two-dimensional calculations of the Parker instability. However, the inclusion of first and higher derivatives of $\langle\boldsymbol{B}\rangle$ in Eq. (5) makes the analysis more susceptible to statistical errors. Brandenburg & Sokoloff (1998) have attempted a more complete analysis including the effects of turbulent diffusion using simulations of accretion disc turbulence. They found that estimating α and γ in the way just described is in fact relatively robust and useful as a first orientation. Hasler et al. (1995) and Brandenburg & Sokoloff (1998) found evidence for nonlocal behaviour, where a whole series of higher derivative terms becomes important. This is beyond the scope of the present paper. As a compromise we have therefore adopted full volume averages, so that derivative terms in Eq. (5) are absent.

We are interested in the exponential growth phase of the instability. Since $\boldsymbol{\mathcal{E}}$ depends on the product of two fluctuating quantities, α and γ will increase proportionally to the *square* of the rms velocity $u_{\rm t}$. Since α and γ have dimensions of velocity, and since the relevant velocity in the system is $v_{\rm A0}$, we present the values of α and γ in units of $v_{\rm A0}\,{\rm Al}^2$, where $\rm Al=\it u_{\rm t}/v_{\rm A0}$ is the Alfvén number of the flow. In models involving flux tubes one may relate $u_{\rm t}$ to the velocity of buoyant flux tubes which, in turn, is limited by turbulent drag forces, so Al should then be a constant somewhat below unity (Parker 1979).

We initialize the runs with a weak solenoidal velocity perturbation consisting of localized eddies with typical initial Mach numbers of 10^{-3}. We normally choose 20 randomly positioned eddies, but the results changed somewhat when we took 100, 200, or 500 eddies. We calculate the values of α and γ for different numbers of initial eddies and use the resulting scatter as an indication of the statistical error of α and γ.

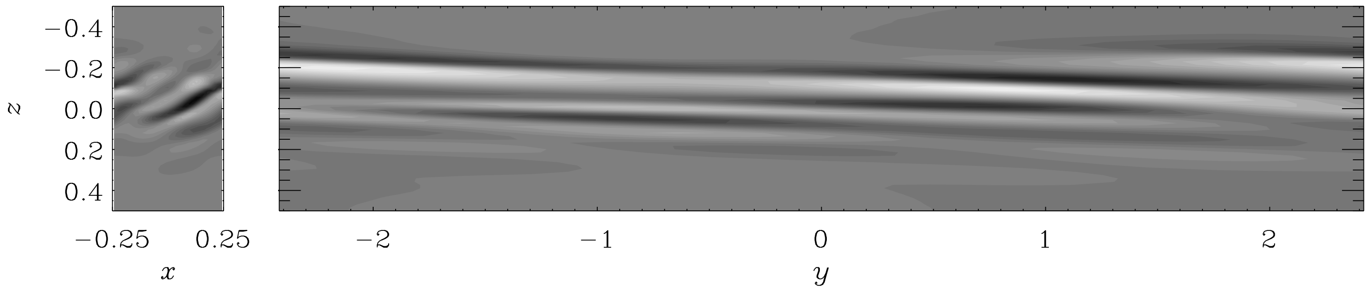

Fig. 1. Grey scale images of arbitrarily chosen xz slice of u_y (left) and yz slice of u_x (right) of the solution for $-30°$ latitude at $t = 20$. The top of the box is at $z = -0.5$. (In the northern hemisphere, the structures in both panels would be tilted the other way around.)

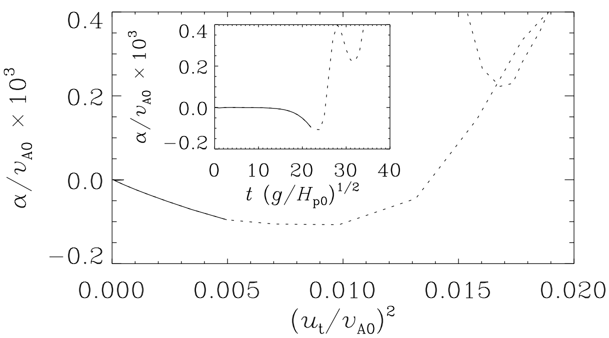

Fig. 2. Example of a plot of α versus u_t for $-30°$ latitude. The solid part of the curve refers to the range where the growth of the solution is exponential. The inset gives the evolution of α as a function of time.

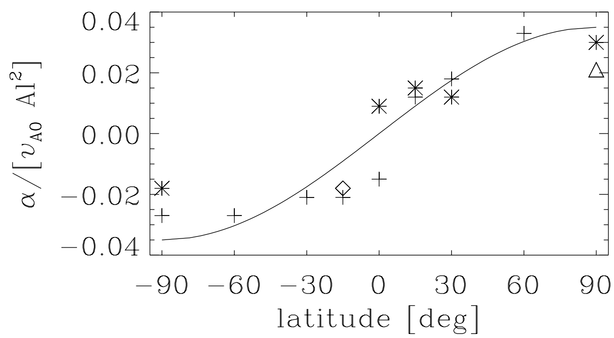

Fig. 3. The latitudinal dependence of the alpha-effect (normalized by $v_{\mathrm{A}0}\mathrm{Al}^2$). The stars refer to initial velocity perturbations using 20 eddies. The plus signs and diamonds refer respectively to 200 and 500 eddies. The solid line represents the fit $\alpha_0 = 0.035 v_{\mathrm{A}0}\mathrm{Al}^2 \cos\theta$. The triangle refers to a run with $v_{\mathrm{A}0}/c_{\mathrm{s}0} = 0.1$ instead of 0.3.

The dependence on initial conditions means that the simulations have not yet settled on the fastest growing eigenfunction before nonlinear effects become important. On the other hand, using weaker initial perturbations still does not remove fluctuations due to hydrostatic adjustment. It is conceivable that we could improve matters by rescaling the results before the solution has reached the nonlinear regime.

3. Results

An example of the eigenfunction at $t = 20$, which is still during the exponential growth phase, is shown in Fig. 1. Note the presence of tilted structures concentrated about $z \approx -0.1$, the unstable top part of the magnetic layer. There are typically 2–4 nodes (1–2 wavelengths) present in the x and y directions, which indicates that the adopted box size is adequately chosen. On the other hand we find more nodes in the vertical direction than suggested by Schmitt's (1994, 1995) analysis. After some time the exponential growth stops and the evolution of α becomes more complicated such that even the sign of α may change. An example of the evolution of α is shown in Fig. 2.

We have carried out a number of simulations for different latitudes and calculated the values of α and γ. The latitude enters the simulation through the Coriolis force. In Fig. 3 we plot the latitudinal dependence of α using different symbols and compare with a simple $\cos\theta$ colatitudinal profile. The agreement is fair, although the scatter is relatively strong, especially near the equator where both positive and negative values of α have been obtained. The extrema of α are found to be not necessarily at the poles, but possibly at somewhat lower latitude.

The value of γ is always negative, corresponding to a mean transport velocity upwards. Its value is $\gamma = -(0.5 \pm 0.2)\, v_{\mathrm{A}0}\mathrm{Al}^2$, but again with significant scatter. There is no clear latitudinal dependence of γ. The growth rate of the instability varies between equator and pole from roughly 0.17 to 0.25.

In Table 1 we give a summary of the dependencies of α on the three input parameters Ω, H_B, and $v_{\mathrm{A}0}$ for runs at $90°$ latitude. Again, since α increases quadratically in the fluctuations we give the ratio $\alpha/\langle \boldsymbol{u}^2\rangle$. Since α is a pseudoscalar, we also give the ratios with other relevant pseudoscalars, the helicity $\langle \boldsymbol{\omega}\cdot\boldsymbol{u}\rangle$ and the current helicity $\langle \boldsymbol{j}\cdot\boldsymbol{b}\rangle$. The trends are clear: $\alpha/\langle \boldsymbol{\omega}\cdot\boldsymbol{u}\rangle$ and $|\alpha/\langle \boldsymbol{j}\cdot\boldsymbol{b}\rangle|$ increase with decreasing field strength and with decreasing scale height of the magnetic field, while $\alpha/\langle \boldsymbol{\omega}\cdot\boldsymbol{u}\rangle$ also decreases with increasing Ω. Furthermore, $\langle \boldsymbol{\omega}\cdot\boldsymbol{u}\rangle$ and $\langle \boldsymbol{j}\cdot\boldsymbol{b}\rangle$ have opposite signs, and the signs of $\alpha/\langle \boldsymbol{\omega}\cdot\boldsymbol{u}\rangle$ and $\alpha/\langle \boldsymbol{j}\cdot\boldsymbol{b}\rangle$ agree with the signs found in BNST. However, it should be noted that the averages are the result of imperfect cancellations and the sign of the helicity tends to change if the average is weighted in favor of regions where the field is strong.

One might expect that α increases with the vertical gradient of the magnetic field. This is indeed the case: lowering the value of H_B from 0.3 to 0.1 leads to an increase of $\alpha/[v_{\mathrm{A}0}\mathrm{Al}^2]$ by at least a factor of ten. Increasing Ω by a factor of three leads to a decrease of $\alpha/[v_{\mathrm{A}0}\mathrm{Al}^2]$ by approximately the same factor. A

Table 1. Summary of parameters for runs at 90° latitude. Comparison of the last two columns shows that $(\Omega H_\mathrm{B}^2 v_\mathrm{A0})^{-1}$ is roughly proportional to $\alpha/\langle\mathbf{u}^2\rangle$.

Run	2Ω	H_B	v_A0	$\frac{\alpha}{\langle\omega\cdot\mathbf{u}\rangle}$	$\frac{\alpha}{\langle\mathbf{j}\cdot\mathbf{b}\rangle}$	$\frac{\alpha}{\langle\mathbf{u}^2\rangle}$	$\frac{1}{\Omega H_\mathrm{B}^2 v_\mathrm{A0}}$
09	1	0.3	0.3	0.007	-0.008	0.07	70
11	1	0.3	0.1	0.02	-0.03	0.2	200
15	1	0.1	0.3	0.10	-0.07	1.0	700
17	3	0.3	0.3	0.002	-0.01	0.03	25

similar behavior was found for an instability of thin magnetic flux tubes (Ferriz-Mas et al. 1994). On the other hand, for small values of Ω there should be no α-effect, so the dependence $\alpha(\Omega)$ should have a maximum at some value which we do not know at present.

4. Conclusions

Our results have shown that in the presence of rotation the magnetic buoyancy instability leads to flows exhibiting an α-effect. The sign of α is positive in the northern hemisphere, and its latitudinal dependence is roughly consistent with a $\cos\theta$ dependence, where θ is colatitude. The latitudinal dependence found here is simpler than the profiles suggested earlier by Schmitt (1985, 1987) using asymptotic theory. A possible cause of the discrepancy could be that the growth rates of the unstable modes are different in the present simulations, which are not in the asymptotic regime considered by him. This is also indicated by the nodal structure of the solution in vertical direction. Another reason might be that the two modes, whose superposition led to the non-monotonic α-profile, do not show up simultaneously in the numerical simulation. This is indicated by the existence of two solutions with values of α of different sign (with approximately zero sum) at the equator and the slight deviation from antisymmetry of α between northern and southern hemisphere. However, more detailed investigations are necessary to clarify these points.

It is important to know the value of α in the nonlinear regime. It is not clear how to estimate α in that case. After the exponential growth phase is over the behavior seems to be rather complicated (Fig. 2). One would expect to approach a (statistically) steady state where Al ($= u_\mathrm{t}/v_\mathrm{A0}$) is approximately constant. If the scaling of α still applies to this case, α would increase with magnetic field strength–in contrast to traditional α-quenching. This idea has recently been invoked to explain the increase in the observed ratio of stellar cycle frequencies to rotation frequencies with magnetic activity (Brandenburg et al. 1998)

In order to keep the buoyancy instability going an unstable field gradient has to be maintained. [This requirement may be relaxed if the field is in a fibral state; see Moss et al. (1998) for corresponding model calculations.] It is unlikely that such a field gradient can be maintained by large-scale dynamo action with magnetically driven α-effect alone, because the instability would diminish the gradient. Instead a separate mechanism may be necessary. For example a combination of turbulent downward pumping of magnetic field (Nordlund et al. 1992) together with field line stretching by vertical shear at the bottom of the convection zone or in the lower overshoot layer may help to produce a concentrated large scale field at the bottom of the convection zone. Preliminary work on overshooting convection with imposed shear (Brandenburg, Stein, & Nordlund, unpublished) shows that strong large scale magnetic field are generated and that the toroidal field profile would indeed sustain magnetic buoyancy instabilities.

Acknowledgements. We thank David Moss, Günther Rüdiger, Anvar Shukurov and Dmitry Sokoloff for useful suggestions and comments on the paper. This work was supported in part by PPARC grant GR/L 30268.

References

Balbus S. A., Hawley J. F., 1991, ApJ 376, 214
Brandenburg A., Sokoloff D., 1998, GAFD (submitted)
Brandenburg A., Nordlund Å., Stein R. F., Torkelsson U., 1995, ApJ 446, 741 (BNST)
Brandenburg A., Jennings R. L., Nordlund Å., Rieutord M., Stein R. F., Tuominen I., 1996, J. Fluid Mech. 306, 325 (BJNRST)
Brandenburg A., Saar S. H., & Turpin C. R., 1998, ApJ 498, L51
Ferriz-Mas A., Schmitt D., Schüssler M., 1994, A&A 289, 949
Hanasz M., Lesch H., 1997, A&A 321, 1007
Hasler K.-H., Kaisig M., Rüdiger G., 1995, A&A 295, 245
Krause F., Rädler K.-H., 1980, Mean-Field Magnetohydrodynamics and Dynamo Theory (Pergamon Press, Oxford)
Moffatt H. K., 1978, Magnetic Field Generation in Electrically Conducting Fluids (Cambridge University Press, Cambridge)
Moss D., Shukurov A., Sokoloff D., 1998, A&A (submitted)
Nordlund Å., Brandenburg A., Jennings R. L., Rieutord M., Ruokolainen J., Stein R. F., Tuominen I., 1992, ApJ 392, 647
Parker E. N., 1955, ApJ 121, 491
Schmitt D., 1984, in: The Hydromagnetics of the Sun, Proceedings of the 4th European Meeting on Solar Physics, ESA SP-220, p. 223
Schmitt D., 1985, Dynamowirkung magnetostrophischer Wellen (PhD thesis, University of Göttingen)
Schmitt D., 1987, A&A 174, 281
Schmitt D., Schüssler M., Ferriz-Mas A., 1996, A&A 311, L1
Steenbeck M., Krause F., Rädler K.-H., 1966, Z. Naturforsch. 21a, 369 See also the translation in Roberts & Stix, The turbulent dynamo..., Tech. Note 60, NCAR, Boulder, Colorado (1971).
Thelen J.-C., 1997, Acta Astron. Geophys. Univ. Comen. XIX, 221